Tribology Letters (2025) 73:68
https://doi.org/10.1007/s11249-025-02002-2

ORIGINAL PAPER

On the Friction and Lubrication of 3D Printed Ti6Al4V Hip Joint Replacement

David Rebenda[1,2] · Lukáš Odehnal[1] · Simona Uhrová[1] · David Nečas[1] · Martin Vrbka[1]

Received: 9 January 2025 / Accepted: 17 April 2025

Abstract

The present study investigates the tribological performance of 3D printed Ti6Al4V total hip replacements (THR) compared to conventionally produced THRs from CoCrMo and FeNiCr alloys. The objective was to evaluate the suitability of 3D printed titanium alloy, with and without DLC coating, for THR rubbing surfaces and to investigate the potential benefits of 3D printing technology for friction and lubrication. A pendulum hip joint simulator was employed to replicate the swinging motion of a hip joint, thereby enabling the measurements of coefficient of friction (COF) and the observation of lubricant film formation under realistic conditions between the metal femoral head and acetabular cup. The experiments demonstrated that additive manufacturing enables the creation of specific surface topographies that can enhance protein adsorption, but also introduce surface imperfections negatively affecting tribological properties. The elevated surface roughness of additively manufactured femoral heads did not inevitably result in an increase in COF and was comparable to that of conventionally manufactured femoral heads. The additively manufactured Ti6Al4V head without DLC coating also exhibited a more rapid increase in lubricant film thickness during dynamic motion. In conclusion, the findings indicate that while 3D printing offers promising advancements in implant customization and material properties, its application requires careful consideration of surface finishing and coating methods to achieve optimal tribological performance.

Graphical abstract

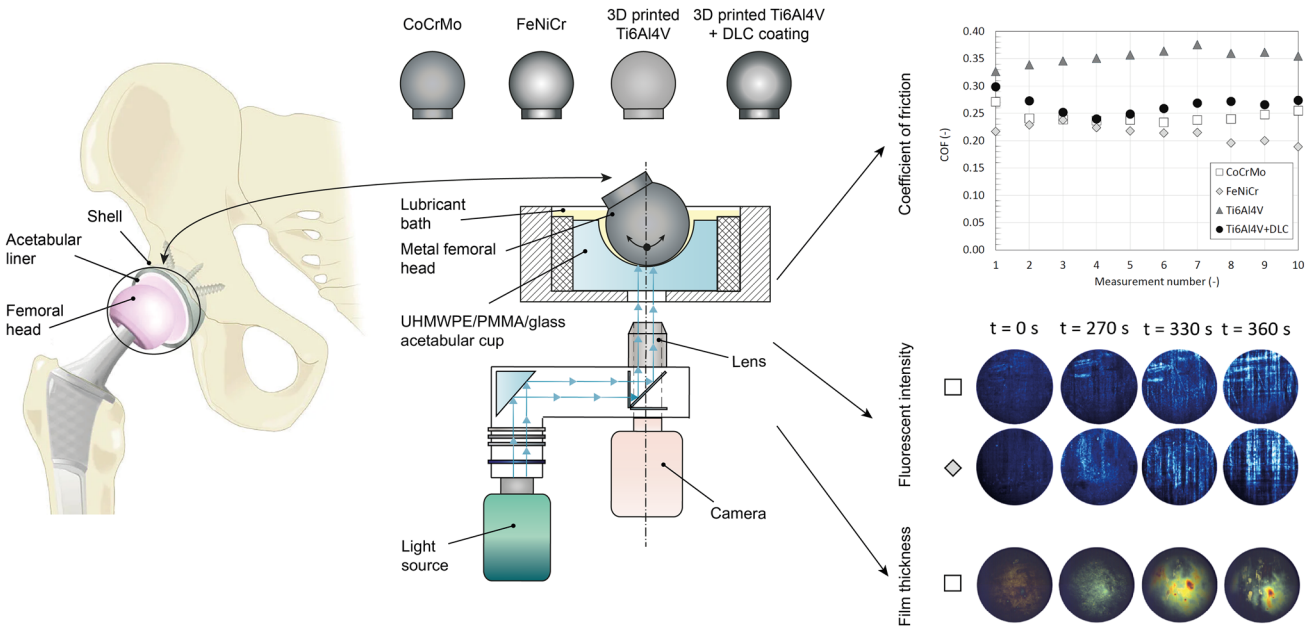

Keywords Total hip replacement · Ti6Al4V · DLC coating · Lubricant film formation · Friction

Extended author information available on the last page of the article

Published online: 28 April 2025

1 Introduction

Total hip arthroplasty (THA) represents a significant advancement in surgical techniques, with millions of individuals reporting enhanced quality of life following the procedure. A common indication for total hip replacement (THR) is a traumatic hip injury or advanced arthritis of the hip. In such cases, the procedure has the potential to significantly alleviate pain and restore mobility. Although THR has a high survival rate of approximately 77.6% at 25 years [1], it can occasionally fail at an earlier point in time [2], which presents a specific risk for younger patients. For patients aged between 50 and 54 years, the estimated lifetime risk of THR revision is up to 29% [3]. Therefore, research focused on improving the durability of THR remains crucial. The longevity of THR is influenced by a number of factors, the majority of which relate to the implant/bone interaction, as well as the wear of the articulating surfaces [4]. When identifying the main cause of implant failure, aseptic loosening due to osteolysis is often recognised as a primary cause [5]. Loosening results from wear particles released from the rubbing surfaces during joint articulation, emphasising the critical role of biotribology in improving implant durability [6]. The wear of articulating surfaces is closely related to the materials of rubbing surfaces.

One of the most widely used groups of materials for THR rubbing surfaces is metal alloys, including stainless steel and CoCrMo. Metal femoral heads or acetabular cups are conventionally manufactured by casting and polishing. However, additive manufacturing (AM) of CoCrMo or titanium alloys represents a progressive method of production, offering numerous potential advantages for THR development. An important focus in additively manufactured THR research is understanding the changes in lubrication, friction, and wear processes in comparison with conventionally produced THR, as these factors could significantly impact the performance and lifespan of the implants. Addressing these challenges through an enhanced understanding of lubrication performance is essential, as insufficient lubrication leads to increased friction and an elevated wear rate, which ultimately determines the lifespan of implant.

Mavraki and Cann [7] were the first to use optical interferometry to measure lubricant film thickness, simplifying THR conditions into a ball-on-disc setup (steel ball and glass disc). They found that the film thickness increased with motion speed for bovine serum (BS), whereas a synthetic protein solution mimicking synovial fluid (SF) showed a more constant film thickness across varying speeds. Subsequent research [8] examined the effects of pressure and temperature, revealing that film thickness rapidly decreased under sliding conditions as proteins were wiped away. Fan et al. [9] replaced the stainless-steel ball with a CoCrMo femoral head to study the effects of speed and lubricant composition under sliding conditions. A thin adhered layer formed quickly, with the film thickness increasing due to hydrodynamic effects, particularly at lower speeds. Myant et al. [10] adopted the same experimental configuration, focusing on the behaviour of key SF proteins, such as albumin and γ-globulin. Static-load experiments showed that γ-globulin formed a more substantial adsorbed layer, while albumin created only a thin layer unaffected by protein concentration. In dynamic tests, both proteins formed agglomerations that periodically increased the film thickness.

The importance of replicating realistic joint movement was later confirmed in studies by Myant et al. [11], who found that transitioning from unidirectional to reversal motion, better mimicking the joint function caused a significant reduction in the lubricant film thickness. The knowledge was summarized in the upcoming study, which presented multiple aspects of the so-called protein aggregation lubrication (PAL) regime, highlighting the main differences against classical elastohydrodynamic lubrication (EHL) theory [12]. To address the issue of surface conformity and contact pressure, Vrbka et al. [13] modified the experimental ball-on-disc setup by a concave glass lens. This adjustment enabled a more accurate representation of lubricant behaviour, showing that conformal contact led to a thicker and more stable lubricant film. To further enhance the importance of contact conformity, the authors later developed a pendulum-based simulator that replicated the actual contact arrangement of a hip joint, introducing a ball-in-cup configuration suitable for in-situ contact observation [14]. The findings confirmed that smaller implants promoted thicker lubricant films, and lower clearances significantly improved lubrication performance [15].

In later studies, Nečas et al. [16] compared BS with model SFs containing albumin, γ-globulin, hyaluronic acid (HA), and phospholipids in concentrations mimicking healthy and pathological SF. It was revealed that the composition and interaction of SF constituents are critical for lubrication, with HA playing a vital role in film formation. To further investigate the role of individual SF constituents within THR lubrication, Nečas et al. [4] developed methodology based on fluorescent microscopy to focus on the performance of stained albumin and γ-globulin. Their experiments revealed that γ-globulin formed a thin, stable layer, while albumin contributed to film enhancement. Further research explored the differences in lubrication mechanisms in hard-on-soft and hard-on-hard implant pairs. Various lubricants were tested, revealing that γ-globulin, HA, and phospholipids interact to form a thin boundary layer, which allows albumin to layer on top [17]. In hard pairs, the lubricant

film tended to thin, while using poly(methyl methacrylate) (PMMA) cups increased film thickness, aligning with previous findings on the sensitivity of SF films to contact pressure. Despite having thicker films, soft pairs showed higher friction, suggesting that internal friction within the lubricant film plays a significant role [18].

Previous research has focused primarily on metal THR components. Vrbka et al. [19] compared the lubrication behaviour of metal and ceramic femoral heads under bovine serum lubrication, examining the influence of speed and the slide-to-roll ratio (SRR). Their results indicated that metal femoral heads generally formed a thicker lubricant film under most conditions. In a subsequent study, Vrbka et al. [20] investigated the COF using a pendulum hip joint simulator, analysing the effects of implant material and diameter for metal-UHMWPE, ceramic-UHMWPE, and ceramic-ceramic pairs. The highest CoF (≈ 0.16) was observed for the metal-UHMWPE pair, while ceramic-UHMWPE showed lower friction (≈ 0.14), with a further decrease (≈ 0.13) for large diameter THR. The lowest friction (0.12) was recorded for the ceramic-ceramic pair, with increased diameter also contributing to the reduction in friction. Another comparison of metal and ceramic THR was made by Necas et al. [21]. The highest friction was found in the metal–metal contact. For the ceramic-ceramic pair, the friction was approximately half that of the metal pair. This behaviour was observed regardless of the applied test fluid. When the polyethylene disc was used as the counterpart to the ceramic ball, the friction was very low, in some cases less than 0.05. Generally, the lowest friction was observed for the ceramic-polyethylene pair.

AM represents a progressive method of production across a wide range of applications, and is also being integrated into the manufacturing process of joint implants [22]. Currently, 3D printing is most commonly utilized in the fabrication of prostheses for the reconstruction of bone segments or entire bones affected by injury, osteomyelitis-induced defects [22], or tumour resection [23]. Moreover, the manufacturing process allows for the creation of a structured implant surface, which facilitates enhanced bone ingrowth, maturation and fixation stability [24].

One of the biocompatible materials suitable for 3D printing is titanium alloy Ti6Al4V. The majority of publications on 3D printed Ti6Al4V alloy have primarily focused on sections of the joint replacements that do not form rubbing surfaces. Nevertheless, a number of studies have initiated this research, offering preliminary insights into this field of investigation. In a study conducted by Grosse et al. [25], a comparison was made between the wear characteristics of CoCr and titanium alloys produced through conventional manufacturing (CM) processes. The findings indicated that the titanium alloy exhibited wear levels that were up to double those observed in the CoCr alloy. Similarly, Odehnal et al. [26] observed comparable results, noting that the Ti6Al4V alloy exhibited significantly higher wear accompanied by the formation of deep grooves. Moreover, the formation of the lubricating film was investigated, and it was found that the Ti6Al4V alloy demonstrated inferior lubricating properties in comparison to the CoCrMo alloy. Other studies have employed experimental methods to compare the properties of AM and CM titanium alloys. A comparison of the percentage of α and β phases reveals significant discrepancies [27] in the relative proportions of these phases. In the case of the CM alloy, the alpha phase represents a mere 25% of the total composition, whereas in the AM alloy, this proportion rises to 75%. Goyal et al. [28] and Bartolomeu et al. [27] conducted experiments in ball-on-disk configuration to compare AM and CM titanium alloys in contact with an Al_2O_3 ball and simulated body fluid (SBF), respectively, with phosphate buffered saline (PBS) as a lubricant. The findings showed that, regardless of the applied load, a reduction in wear was consistently observed for the AM alloy. This is attributed to the presence of harder microstructural constituents, which are formed during production through the utilization of a high cooling rate. Moreover, Goyal's [28] experiments demonstrated a reduction in the coefficient of friction (CF) for all forces. In contrast, Bartolomeu [27] reported that a notable difference in friction was not apparent.

Although it has been demonstrated that the use of AM has resulted in enhanced wear characteristics, there is still a lack of comprehensive characterization of the tribological behavior of the AM titanium alloy in the frictional contact. It may therefore be necessary to employ a coating in order to optimize the performance of the alloy. Diamond-like carbon (DLC) is the most prevalent coating material used for articular implants, which offers a crucial benefit of reducing the wear rate. However, the DLC coating can also have a negative impact on the human body, particularly in terms of the delamination [29] that can occur. Consequently, efforts have been made to identify an appropriate interlayer [30, 31] or finishing operation to be applied to the substrate material [32] in order to enhance its behaviour and prevent potential issues.

In addition to additively manufactured metal components, DLC can also be applied to polymer components. Xie et al. [33] deposited a-C:H coating on UHMWPE resulting in increased hardness (0.139 GPa compared to 0.010 GPa of the UHMWPE substrate), scratch resistance and wear resistance. Improved wear resistance of a-C:H coated UHMWPE against Al_2O_3 ball mating surfaces was also reported by Puértolas et al. [34], although higher COF was observed compared to uncoated UHMWPE. Increased COF due to an a-C:H coating on a UHMWPE substrate was also reported by Rothammer et al. [35, 36], with the authors attributing this behaviour to coatings having higher surface roughness

compared to the uncoated substrates. However, the wear of UHMWPE was significantly reduced, reaching up to 49% reduction against CoCr and 77% reduction against Ti6Al4V. In another study, Rothammer et al. [37] investigated the wear resistance of ta-C coatings. In sliding experiments using metal pin on UHMWPE disc configuration, the disc wear rates were reduced by 48% (against CoCr) and 73% (against Ti6Al4V) compared to uncoated pairings. Similarly, pin wear rates were reduced by a factor of 20 (CoCr) and 116 (Ti6Al4V).

The lubrication of THR is a complex process, the outcome of which is influenced by a number of factors. These include the material used for the femoral head and acetabular cup, implant geometry, surface conformity, SF composition, motion dynamics, and so forth. The ongoing research in this area is contributing to a refinement of our understanding of lubrication processes, which may identify potential areas for improvement in future THRs. The advent of additive manufacturing technologies gives rise to novel research questions, particularly in the context of 3D printing of biocompatible materials such as the Ti6Al4V alloy. It prompts the inquiry of whether a 3D printed femoral head can serve as a rubbing surface for a THR. It is therefore pertinent to ask whether the tribological properties of a 3D printed Ti6Al4V femoral head are comparable to those of conventionally manufactured THRs made from stainless steel or CoCrMo alloys. In addition, it is worth investigating whether its tribological behaviour can be improved in any way, for example, by applying a coating to the rubbing surfaces. In order to respond to these questions, the present study aims to conduct a comprehensive tribological assessment of a conventionally produced metal femoral heads and a 3D printed Ti6Al4V femoral heads with or without a DLC coating in a realistic ball-in-cup configuration. The pendulum hip joint simulator, together with the optical interferometry and fluorescent microscopy apparatus, will be utilised to analyse the COF and lubricant film formation in the contact between the CoCrMo, FeNiCr or Ti6Al4V femoral heads and the ultra-high-molecular-weight polyethylene (UHMWPE), PMMA or glass acetabular cup.

2 Materials and Methods

2.1 Experimental Setup

In order to replicate the swinging motion of a hip joint, a pendulum hip joint simulator (Fig. 1) was utilized to conduct frictional measurements and observations of lubricant film formation. The simulator comprises a static frame that holds a pot with an acetabular cup fixed with a resin, and a movable frame (pendulum). The femoral head is attached to the movable frame, which applies a load on the femoral head and enables the swinging motion between the femoral head and the acetabular cup. The range of swinging motion is limited by the simulator design and is $\pm 16°$, which corresponds to the range of flexion–extension motion in a human hip. The frequency of the swinging motion is approximately 0.5 Hz, which is closely comparable to the slow pace of gait observed in elderly people.

In order to observe the formation of the lubricant film, two distinct optical techniques were utilized. The first method, fluorescence microscopy, permits the separation and observation of individual constituents of SF (albumin, γ-globulin, HA), so their role in lubricant film formation can be clarified. The principle of fluorescence phenomena involves three stages. Initially, photons are excited by the light source and subsequently absorbed by the fluorescent

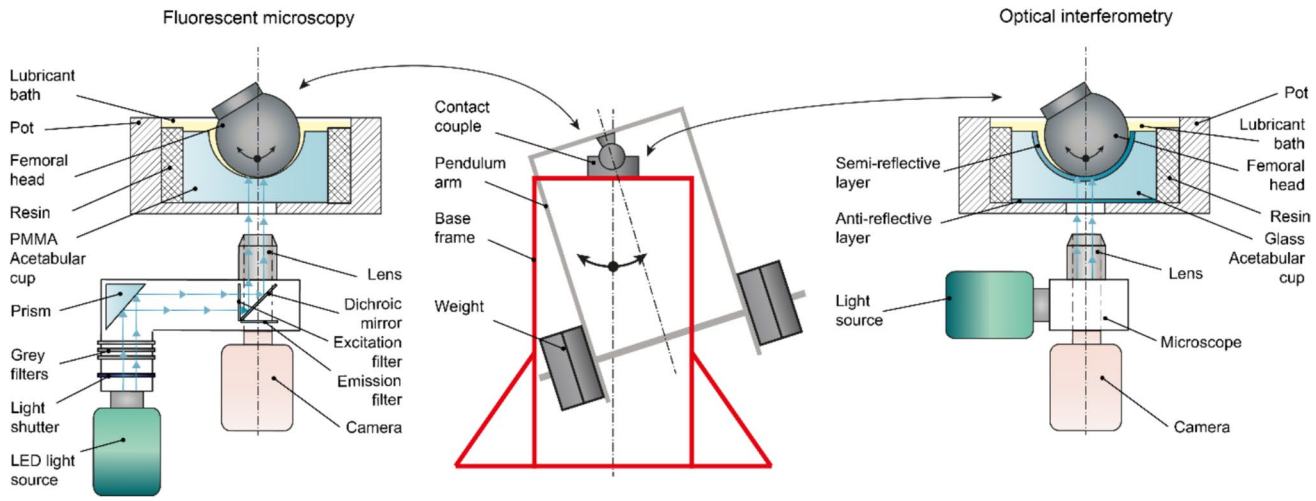

Fig. 1 Experimental apparatus

dye within the tested lubricant. This phase is called excited-state lifetime, lasts 1–10 ns, while the molecule undergoes relaxation. This results in partial energy dissipation, which enhances the fluorescence emission. Consequently, the emitted photons have lower energy, causing the emitted radiation to have a longer wavelength than the excited radiation. This shift allows for the separation of excitation and emission, enabling the determination of the fluorescence yield.

For fluorescence measurements, the pendulum simulator was enhanced with the incorporation of a bespoke microscope, as illustrated schematically in Fig. 1 (left). The contact area was illuminated by a light-emitting diode, and the light passed through a set of optical filters to achieve the required wavelength of emitted and excited light. The data obtained from the in-situ observations were recorded with a high-speed complementary metal-oxide semiconductor (CMOS) camera, the Andor Neo 5.5 (Andor, Belfast, UK). As a counter surface to the metal femoral heads, a transparent PMMA acetabular cup was used. PMMA was selected for its transparency and to mimic the mechanical properties of the UHMWPE acetabular cup, a commonly used material in orthopaedics. The functionality of the apparatus had already been validated and described in more detail in a previous publication by Nečas et al. [17].

To obtain specific information about lubricant film thickness, a fluorescence microscope was replaced with an optical interferometry apparatus (Fig. 1 (right)). This configuration comprised a high-speed digital camera Phantom v710 (Vision Research, Wayne, NJ, USA), an optical microscope, and a light source. The apparatus has been validated and described in detail in previous studies [14, 15]. The PMMA acetabular cup was replaced by a BK7 glass cup, which was coated with an anti-reflective layer on the bottom and a semi-reflective chromium layer on the frictional surface to enhance the contrast of interference fringes. The glass cup was selected for its transparency and suitability for achieving optimal coating adhesion.

2.2 Materials

Femoral heads, machined in both additive and conventional ways, were tested. Conventional methods, namely casting and polishing, were employed to produce CoCrMo (ASTM-F75) and FeNiCr (ISO 5832-1) alloy samples. Ti6Al4V (ISO 5832-3) samples, with or without a DLC coating, were manufactured using the SLM 3D printing method, followed by conventional surface finishing. All femoral heads were produced by ProSpon (Kladno, Czechia), certified producer of Ti6Al4V 3D printed bone implants and joint replacements. The DLC coating was applied by HVM PLASMA (Prague, Czechia) using plasma-assisted chemical vapor deposition (type: Cr + W–C:H + DLC, hardness 2 000 HV, adhesion HF2). Prior to the experiments, the geometry of all femoral heads was evaluated using an optical 3D scanner, the ATOS Triple Scan (GOM, Braunschweig, Germany), in order to analyse the exact diameter and to identify any deviations from an ideal spherical shape. The nominal diameter of the femoral heads was 28 mm, whereas the 3D scanner measured a real diameter of a 27.98 mm for all four femoral heads. The 3D scans of the femoral heads are presented in Fig. 2 (left column).

Additionally, the surface topography of the samples was evaluated. The surface roughness (*Sa*) was determined using a Bruker Contour GT-X8 optical profilometer (Bruker, Billerica, MA, USA), which employs phase-shifting interferometry. Each femoral head was measured five times on different parts of the surface, with each evaluated area set to 0.4×0.55 mm. The mean surfaces roughness of the femoral heads was as follows (mean ± standard deviation): 7.19 ± 0.62 nm for CoCrMo, 11.46 ± 2.33 nm for FeNiCr, 34.21 ± 4.59 nm for Ti6Al4V and 50.10 ± 15.44 nm for Ti6Al4V + DLC. Figure 2 (middle and right column) illustrates typical greyscale images of the surface and surface roughness measurements for each femoral head.

Lastly, the wettability of the femoral heads was characterized using the sessile drop technique, whereby the contact angle between the femoral head surface and a drop of model SF (described subsequently) was measured. The results are presented in Fig. 3.

As counter-surfaces to the femoral heads, UHMWPE, PMMA, and BK7 glass acetabular cups were used. The UHMWPE cup was selected for analysis of friction in realistic material combinations, while the PMMA and BK7 cups were necessary for in-situ observation of the contact area using fluorescence microscopy and optical interferometry. As with the femoral heads, the acetabular cups were scanned with a 3D scanner to measure the nominal diameter of the spherical surface, and an optical profilometer was used to analyse surface roughness. The results are presented in Table 1.

As a lubricant, model SF was prepared in accordance with methodology outlined by Galandaková et al. [38]. PBS was used as the basic solution, with the following additions: bovine serum albumin (BSA, Sigma Aldrich A7030, St. Louis, MO, USA), γ-globulin from bovine blood (BSG, Sigma Aldrich G5009, St. Louis, MO, USA), hyaluronic acid (HySilk, Contipro, Dolní Dobrouč, Czechia) and L-α-phosphatidylcholine (Sigma Aldrich P3782, St. Louis, MO, USA). The concentrations reflected those found in the SF of healthy individuals, specifically: albumin 20 mg/ml, γ-globulin 3.6 mg/ml, HA 2.5 mg/ml and phospholipids 0.15 mg/ml. For the purpose of measurements using the fluorescent microscope, the individual components of the model SF were labelled with fluorescent dyes. Albumin was labelled with Rhodamine B isothiocyanate (RBITC, Sigma Aldrich 283,924, St. Louis, MO, USA), while γ-globulin

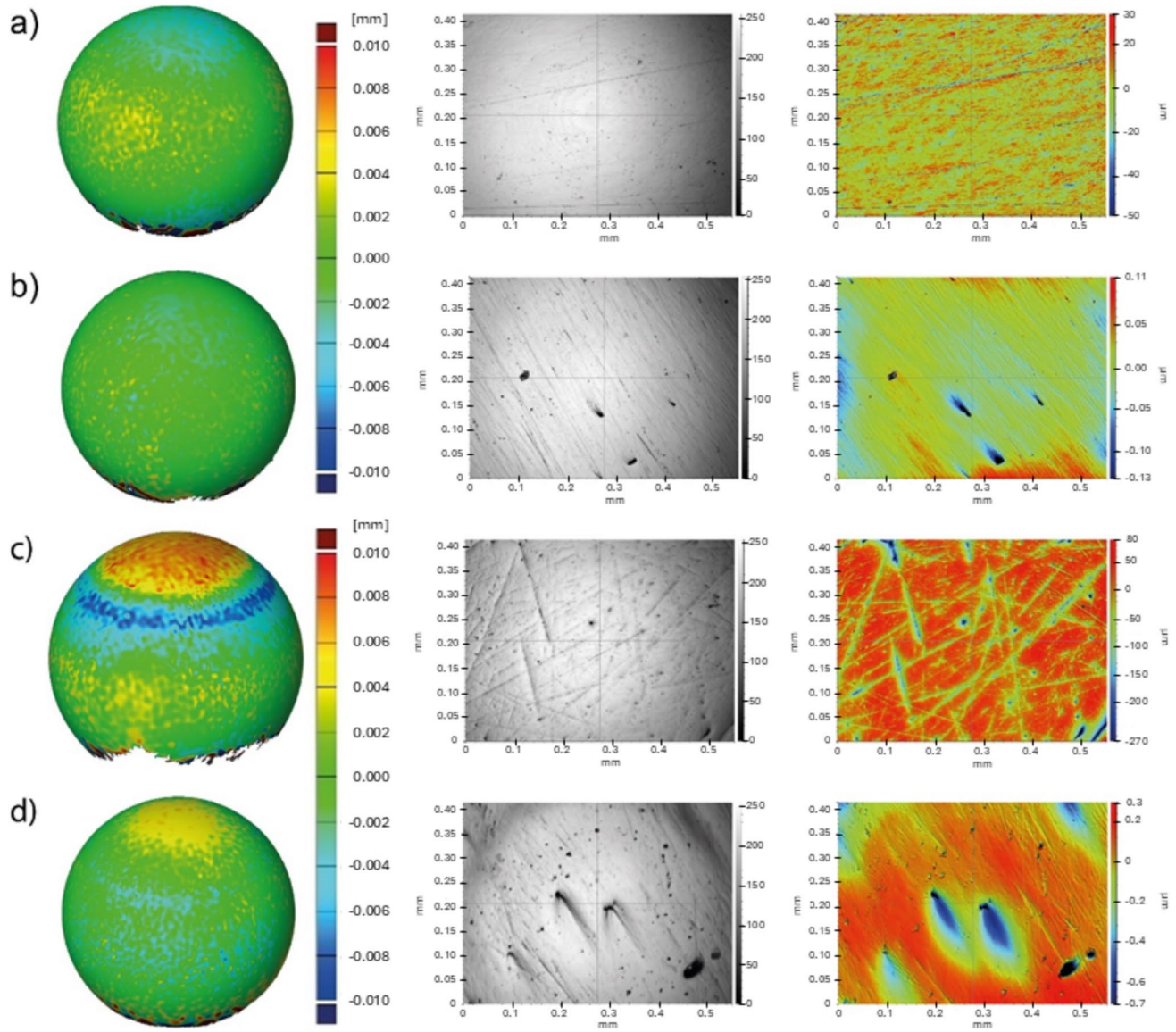

Fig. 2 3D scan, surface image and typical surface roughness measurements results for femoral heads made from: **a** CoCrMo, **b** FeNiCr, **c** Ti6Al4V, **d** Ti6Al4V + DLC

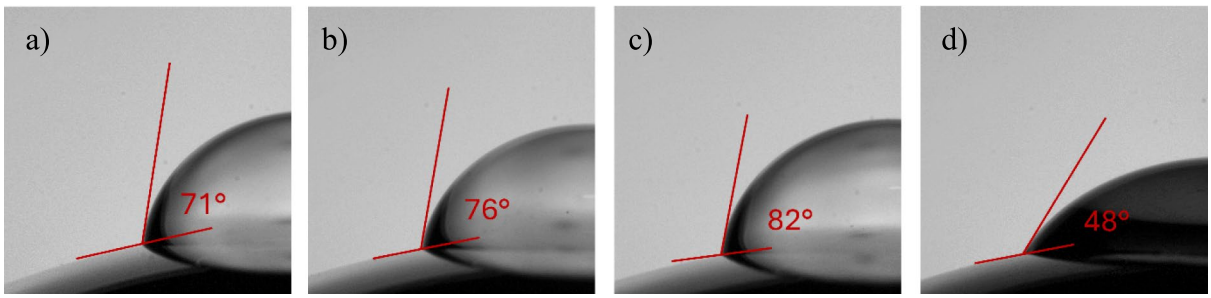

Fig. 3 Contact angles for femoral heads measured with model SF: **a** CoCrMo, **b** FeNiCr, **c** Ti6Al4V, **d** Ti6Al4V + DLC

Table 1 Characteristics of acetabular cups

Material	Experiment	Diameter (mm)	Diametric clearance (μm)	Surface roughness (Sa) [nm]
UHMPWE	COF measurement	28.22	240	2709 ± 140
PMMA	In-situ observation by fluorescent microscopy	28.11	130	15.6 ± 0.44
BK7 glass	In-situ observation by optical interferometry	28.05	70	3.6 ± 0.09

Table 2 Values of contact pressures

Material	BK7 glass cup contact pressure (MPa)	PMMA cup contact pressure (MPa)	UHMPE cup contact pressure (MPa)
CoCrMo	24.1	5.1	2.4
FeNiCr	–	5.1	2.4
Ti6Al4V	21.1	5.1	2.4
Ti6Al4V + DLC	–	5.1	2.4

and hyaluronic acid were labelled with fluorescein isothiocyanate (FITC, Sigma Aldrich F7250, St. Louis, MO, USA).

2.3 Test Conditions and Results Evaluation

All tests were conducted under fully flooded conditions using model SF. The temperature of the contact bodies was maintained at 37° throughout the measurements. A load of 532 N was applied by dead weight on the contact bodies, resulting in varying contact pressure values depending on the material of the ball and cup. The exact contact pressure values for each material combination were determined through the application of Hertzian theory and are presented in Table 2.

Firstly, the COF between femoral heads and the UHMWPE cup was measured through the implementation of the following methodology: the pendulum frame was meticulously deflected by 16° and subsequently released, thereby enabling spontaneous damped oscillatory motion to occur. The angular velocity of the pendulum arm was monitored using an accelerometer. The measurement was repeated 10 times conclusively without unloading the contact. The data were processed using MATLAB software (MathWorks, Inc., CA, USA), with the peaks of the angular velocity fitted with a linear function as described in a study by Crisco et al. [39], and the COF values calculated.

In order to simulate the standing and walking phases of the gait cycle, a combined kinematics approach was employed for both fluorescence microscopy and optical interferometry (Fig. 4). The initial phase entailed the cyclic loading and unloading of the static contact. A total of ten cycles were performed, comprising a ten-second loaded phase and a twenty-second unloaded phase. Subsequently, a 60-s relaxation period was conducted under loaded conditions. In the second phase, the pendulum arm was deflected by 16° and released to initiate spontaneous damped oscillation, as was done during the frictional measurements. The third phase comprised maintaining the contact under static loaded conditions for a further 300 s, allowing for the observation of the relaxation of the lubricant film.

The film thickness values were evaluated from the optical interferometry images and videos, while the fluorescent intensity values were measured from the fluorescence microscopy videos and images. Fluorescent intensity values were normalized in order to account for variations in the initial settings of the light source, microscope filters and used fluorescent markers, which can influence the initial

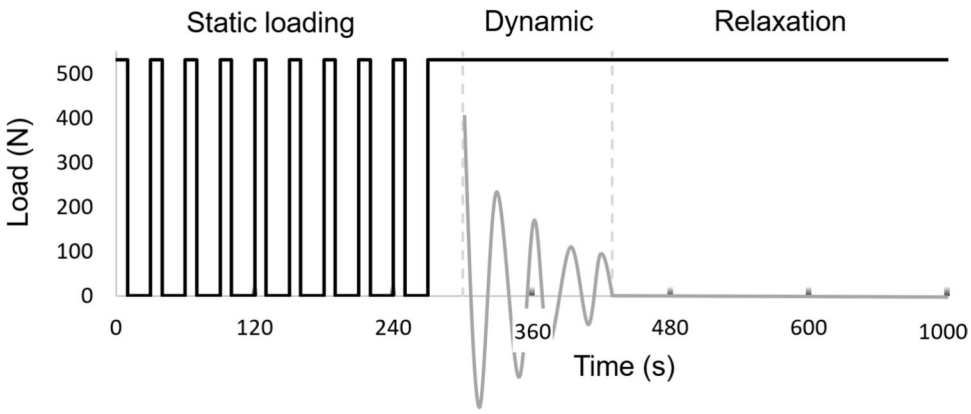

Fig. 4 Kinematic conditions of the tests

fluorescent intensity. In order to ensure comparability across experiments, the initial fluorescent intensity was set to 1 000 by dividing the starting value by a constant, after which all subsequent data from the experiment were divided by this constant. This normalization method has been previously used and validated in our earlier study [17].

3 Results

3.1 Friction

Figure 5 shows the results of the COF measurements performed between the four investigated femoral heads and the UHMWPE acetabular cup. The COF values reported for three of the four tested femoral heads (CoCrMo, FeNiCr and Ti6Al4V) were found to be highly similar. No discernible trend was identified in the COF measurement outcomes for CoCrMo and FeNiCr. In contrast, a slight increase in COF values from 0.047 to 0.058 was observed for Ti6Al4V during the initial five measurements, followed by a period of steady-state values during the remainder of the measurement. Furthermore, the CoCrMo and Ti6Al4V exhibited identical average COF values following ten consecutive measurements, with a value of 0.056. The FeNiCr exhibited the lowest average COF, at 0.048 ± 0.004. Conversely, the Ti6Al4V head coated with a DLC layer exhibited COF values that were over twice as high as those of the other specimens, with an average of 0.137 ± 0.002. The results of individual measurements reported an initial increase in COF from 0.132 to 0.137, after which the COF values were stabilized.

To compare a realistic material combination (metal femoral head and UHMWPE cup) and a hip joint replacement model used for in-situ studies of lubricant film formation, frictional maseruements between all four metal femoral heads and PMMA cup, which was lately used for measurement with fluorescent microscopy, were conducted. The results of these measurement are shown in Fig. 6. In comparison with UHMWPE, PMMA exhibited a COF value that was multiple times higher. The lowest average value of COF was observed once more for the FeNiCr, with a value of 0.214 ± 0.014. The results of the individual measurements demonstrated a slight increase in COF from 0.217 to 0.238 during the initial three measurements, followed by a gradual decrease to 0.189 during the remaining measurements. The CoCrMo exhibited an average COF value of 0.244 ± 0.011. With the exception of the initial measurement, the results of the individual measurements exhibited minimal variation, with a slight increase from 0.234 to 0.255 observed during the final five measurements. In contrast with the findings for the UHMWPE cup, the impact of the DLC coating on the friction of the 3D printed Ti6Al4V was reversed. The 3D printed Ti6Al4V femoral head with DLC coating exhibited resutls that were more closely aligned with those of the convenionally manufactured specimens (CoCrMo, FeNiCr) than the Ti6Al4V head without DLC coating, with an average COF value of 0.265 ± 0.016. The individual measurements demonstrated a notable decline in COF from 0.299 to 0.240, during the initial four mesaurements. This was follwed by an increase to 0.274 during the remaining measurements. The highest average value of COF was observed for the 3D printed Ti6Al4V specimen without DLC coating, with an average of 0.354 ± 0.013. The results demonstrated

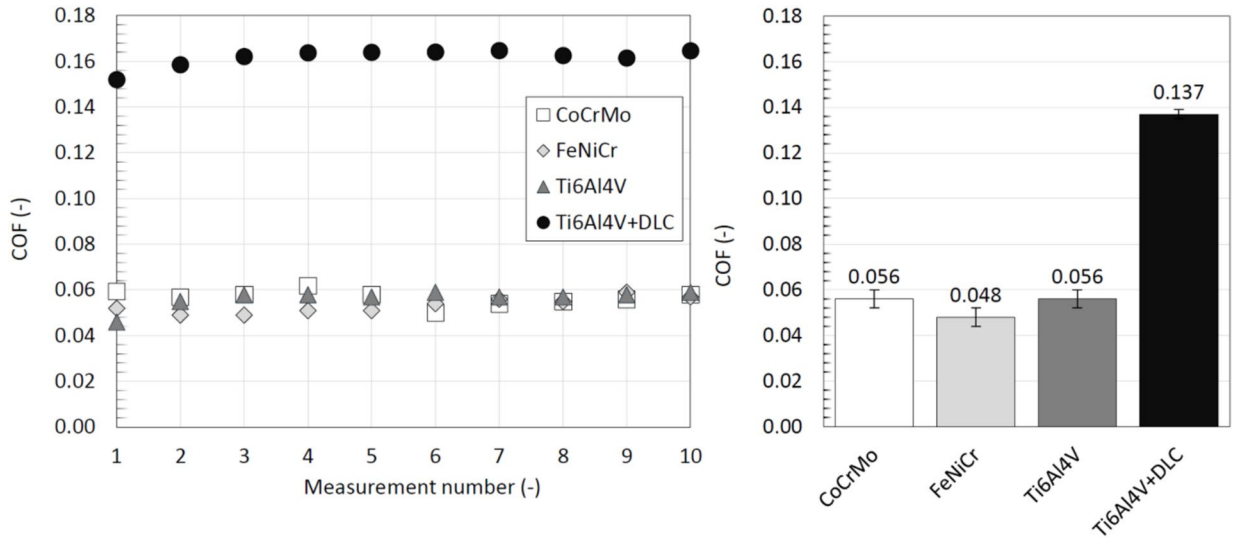

Fig. 5 COF between the tested femoral heads and UHMWPE cup: results of individual experiments with each metal femoral head (left), mean values and standard deviations for each femoral head material (right)

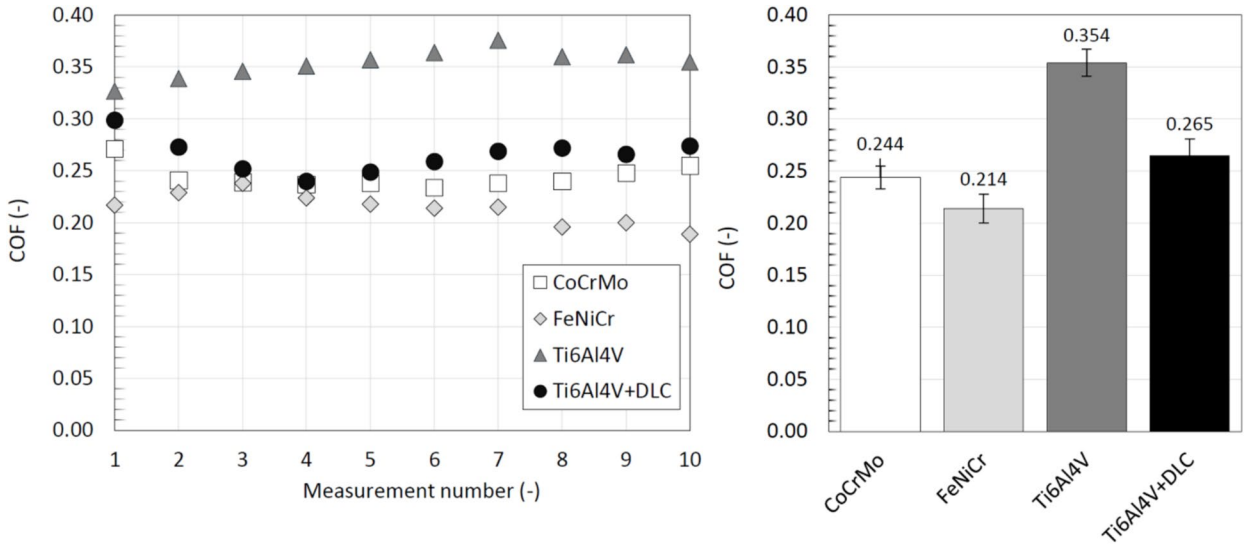

Fig. 6 COF between the tested femoral heads and PMMA cup: results of individual experiments with each metal femoral head (left), mean values and standard deviations for each femoral head material (right)

a gradual increase from 0.327 to 0.376 in the initial seven measurements, followed by a decrase to 0.355 in the remaining measurements.

3.2 Observation of Individual SF Constituents

The first series of in-situ measurements was focused on the role of individual SF constituents in lubricant film formation. A fluorescence microscope was attached to the pendulum hip joint simulator and albumin, γ-globulin and HA were sequentially labelled with a fluorescent dye. Fig. 7 shows the results of the measurements with SF containing fluorescently labelled albumin, with the fluorescent intensity (dimensionless film thickness) as a function of time. During the first phase of the experiment, which consisted of cyclic loading and unloading of the static contact, the fluorescent intensity increased for all four femoral heads, caused by the formation of a boundary adsorbed film composed of albumin, as can be seen from the images of the contact area taken during the experiments. The initial fluorescent intensity value has been normalized and is therefore the same for all femoral heads. The steepest increase in fluorescent intensity during static loading was reported for Ti6Al4V and the least steep increase was reported for Ti6Al4V with DLC coating. The fluorescent intensity values for individual femoral heads at the end of static loading were as follows: 1639 for Ti6Al4V, 1587 for FeNiCr, 1412 for CoCrMo and 1233 for Ti6Al4V + DLC.

Involvement of the swinging motion resulted in an increase in albumin fluorescent intensity except for CoCrMo, which may have been caused by the damage to the adsorbed protein layer during extension of the pendulum frame. Individual femoral heads then showed different trends in fluorescent intensity during the pendulum swinging motion. Overall, the lowest fluorescent intensity was reported for CoCrMo, while fluorescent intensity gradually increased during the first half of the measurement and then stabilized for the remainder of the measurement. At the end of swinging motion, the fluorescent intensity for CoCrMo was 1509. The second lowest fluorescent intensity values were measured for Ti6Al4V, while the progression was almost constant, with fluorescent intensity values fluctuating between 1684 and 1724. FeNiCr showed an initial increase of fluorescent intensity during the first few seconds, followed by a slight decrease. At the end of swinging motion, fluorescent intensity for FeNiCr was 1808. The swinging motion of FeNiCr also lasted the longest, leading to the lowest COF between this femoral head and the PMMA acetabular cup. The highest values of fluorescent intensity, 2584 at the end, were reported for Ti6Al4V, while the data show a large fluctuation, probably caused by protein agglomerates entering and leaving the contact area during the swinging motion. The final stage of the experiment, focusing on albumin boundary layer relaxation, showed a decrease in fluorescent intensity for CoCrMo, FeNiCr and Ti6Al4V + DLC femoral head and an increase for Ti6Al4V. At the end of the measurement, the fluorescent intensity values were (from highest to lowest) – 3101 for Ti6Al4V, 1648 for FeNiCr, 1554 for Ti6Al4V + DLC and 1464 for CoCrMo.

The second set of measurements was performed with SF containing fluorescently labelled γ-globulin. The results in Fig. 8 show that this time FeNiCr achieved the highest fluorescent intensity values at the end of the static loading/unloading phase – 1145. As in the case of the albumin

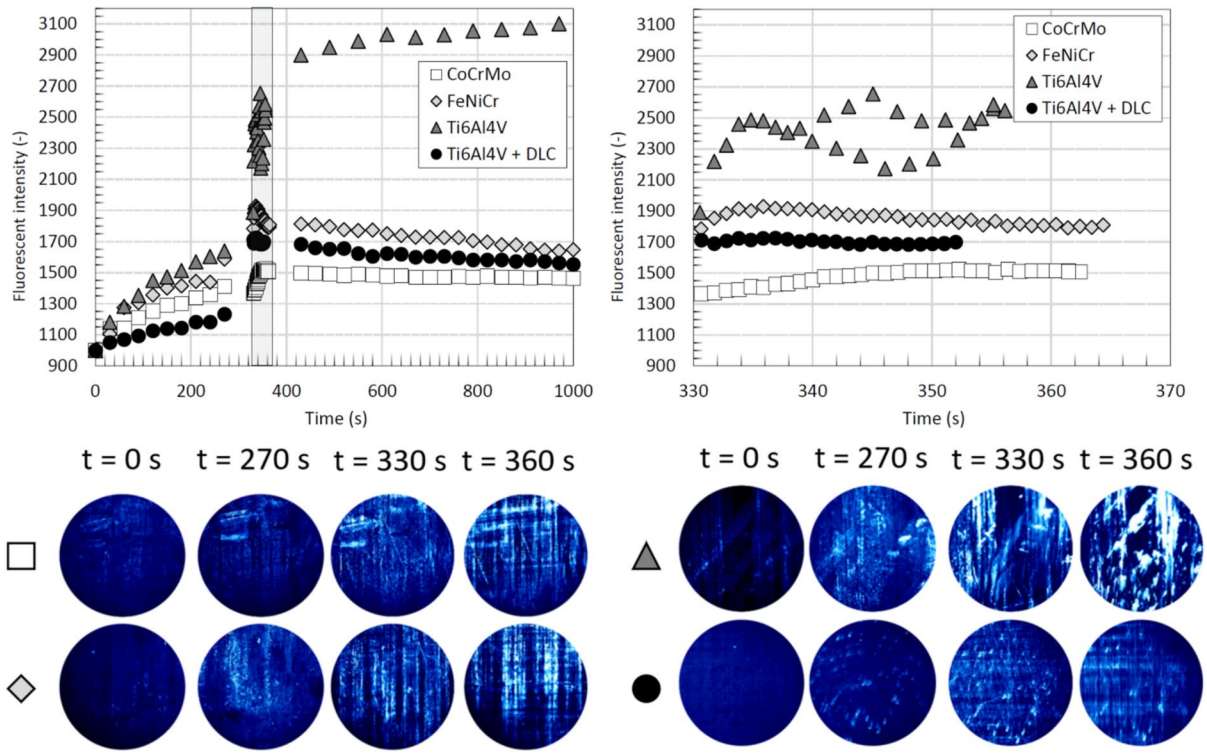

Fig. 7 Time-dependent development of fluorescent intensity for all four tested femoral heads during measurements with SF containing fluorescently labelled albumin (top), images of the contact area taken during the experiments (bottom)

measurements, FeNiCr was followed by a CoCrMo and Ti6Al4V + DLC with fluorescent intensity values of 1077 and 1040 respectively. Contrary to the result with albumin, Ti6Al4V showed the lowest fluorescent intensity value at the end of the static loading phase. The fluorescent intensity increased initially, but at the end of the static loading it was almost the same as at the beginning of the test, indicating that γ-globulin was not part of the adsorbed protein layer or that no boundary lubricating layer was formed.

During the second phase, when the pendulum was swinging, Ti6Al4V reported the steepest increase in fluorescent intensity and at the end of this phase it reported the highest value of fluorescent intensity of all the femoral heads tested – 1260. Ti6Al4V + DLC showed moreless constant values of fluorescent intensity, fluctuating between 1004 and 1031, as in the case of measurements with fluorescently labelled albumin. Both conventionally manufactured femoral heads—CoCrMo and FeNiCr—showed a slight decrease in fluorescent intensity. The final relaxation part resulted in a gradual decrease in fluorescent intensity for all femoral heads tested. At the end of the measurement the fluorescent intensity was 1179 for Ti6Al4V, 990 for Ti6Al4V + DLC, 986 for FeNiCr and 934 for CoCrMo.

The final set of in-situ fluorescent microscopy observations was made with SF containing labelled HA. The results in Fig. 9 showed a gradual increase in fluorescent intensity for all femoral heads as in the case of albumin. However, this time only a slight increase was observed, which was almost identical for all femoral heads. At the end of static loading, the fluorescent intensity for individual femoral heads was between 1038 and 1095, with the highest value measured for CoCrMo and the lowest for Ti6Al4V + DLC. During the pendulum swinging motion, the fluorescent intensity did not change significantly for most samples. CoCrMo and Ti6Al4V + DLC showed an almost constant progress with quite similar fluorescent intensity values. For CoCrMo, the fluorescent intensity fluctuated between 1051 and 1093 and for Ti6Al4V + DLC between 1033 and 1092. The only femoral head that showed an increase in HA fluorescent intensity during swinging motion was Ti6Al4V. The fluorescent intensity increased from 1093 to 1183. The damped swinging motion between the Ti6Al4V femoral head and PMMA cup also lasted the shortest time, elicited the highest COF in the contact during motion. The longest swinging motion, i.e. the lowest COF in contact, was reported for FeNiCr. FeNiCr also reported a decrease in HA fluorescent intensity from 1141 to 1085. The final relaxation phase again resulted in a decrease in fluorescent intensity for all femoral heads tested. The most significant decrease was observed for Ti6Al4V, which reduced the increase in fluorescent intensity during the swinging motion and approached the final fluorescent intensity value closer to the rest of the femoral heads tested.

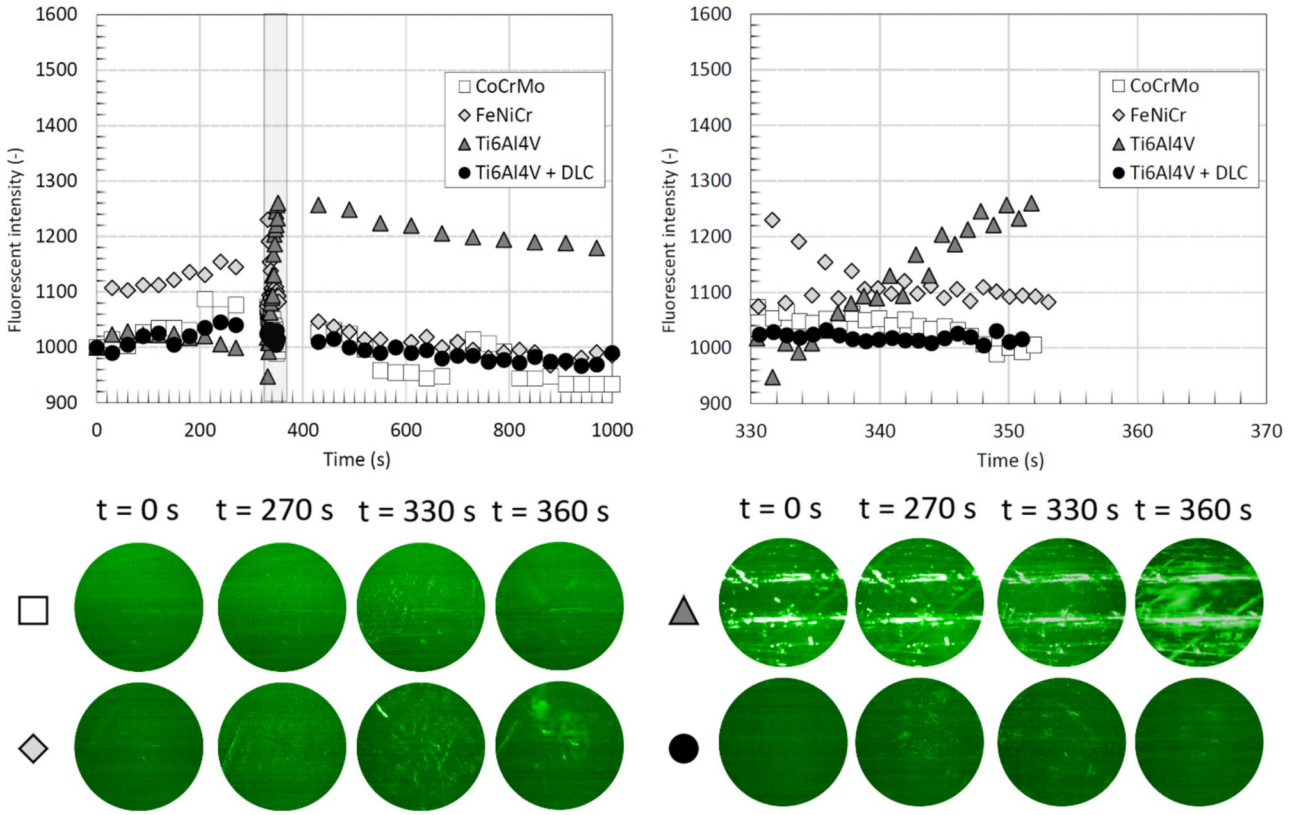

Fig. 8 Time-dependent development of fluorescent intensity for all four tested femoral heads during measurements with SF containing fluorescently labelled γ-globulin, images of the contact area taken during the experiments (bottom)

The final fluorescent intensity values were quite close for all femoral heads – 1014 for Ti6AL4V + DLC, 1010 for Ti6Al4V, 993 for FeNiCr and 963 for CoCrMo.

3.3 Film Thickness Measurements

In order to obtain information regarding the film thickness between the femoral head and acetabular cup contact, the fluorescent microscope was replaced with an optical interferometry apparatus (Fig. 1). Additionally, the PMMA cup was replaced with a BK7 glass acetabular cup that had been coated with an anti-reflex and chromium layer. The same measurement methodology, consisting of static loading, dynamic swinging part and lubricant film relaxation phase, was applied. In this investigation, only CoCrMo femoral head, which is the most commonly used conventionally produced metal femoral head, and the Ti6Al4V femoral head, which is representative of the emerging generation of 3D printed femoral heads, were tested. The results are presented in Fig. 10. As with the observation of contact by fluorescent microscopy, the cyclic loading and unloading of the static contact resulted in the formation of an adsorbed boundary layer and a gradual increase in the film thickness for both femoral heads. Following 10 cycles, the film thickness was observed to be 89 nm for the Ti6Al4V femoral head. CoCrMo femoral head exhibited film thicknesses of 54 nm. During the swinging phase, a notable increase in film thickness was observed in comparison to the static loading and unloading cycles for both the CoCrMo and Ti6Al4V. However, the evolution of the lubricant film thickness for both femoral heads exhibited notable differences. While the CoCrMo exhibited a gradual loss of lubricating film thickness during the swinging motion, the Ti6Al4V initially demonstrated a steep increase in film thickness, followed by a decrease when the motion slowed. Furthermore, the extent of change in thickness was found to vary considerably between these two samples. In the case of CoCrMo, the film thickness exhibited a gradual decrease from 138 to 73 nm. In contrast, Ti6Al4V initially displayed an increase from 252 nm up to 467 nm, followed by a subsequent decrease to 287 nm. Furthermore, it can be observed that the movement ceased much earlier for Ti6Al4V, at 14 cycles compared to 50 for the CoCrMo. This is associated with the elevated COF in the contact. In the final phase of the experiment, where the adsorbed boundary layer was maintained under static loading, only a slight reduction in film thickness was evident for both CoCrMo and Ti6Al4V.

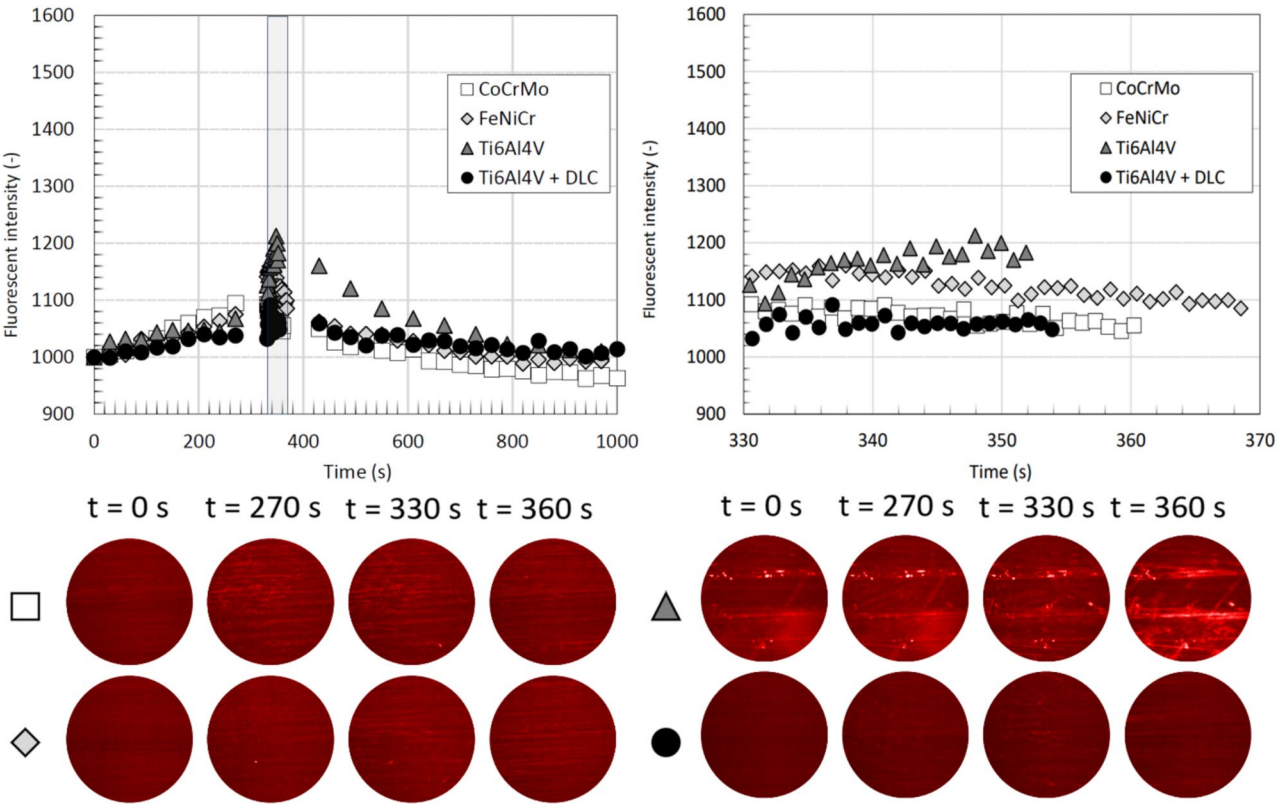

Fig. 9 Time-dependent development of fluorescent intensity for all four tested femoral heads during measurements with SF containing fluorescently labelled HA, images of the contact area taken during the experiments (bottom)

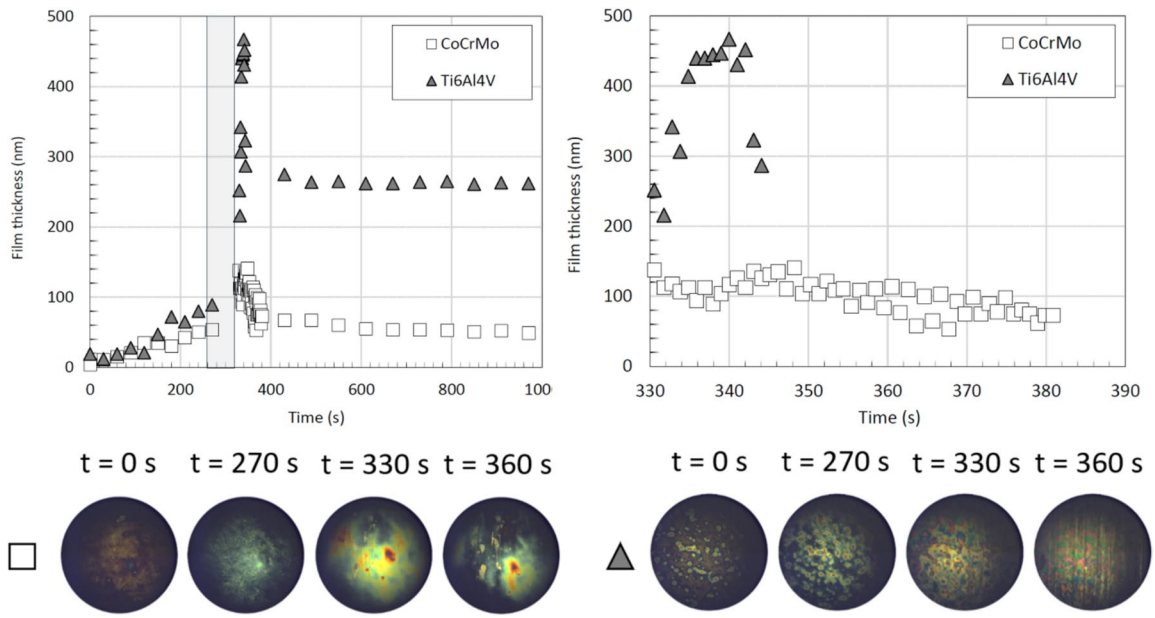

Fig. 10 Time-dependent development of film thickness for CoCrMo and Ti6Al4V femoral heads (top), chromatic interferograms taken during the experiments (bottom)

4 Discussion

4.1 General Discussion

The present study offers insight into the frictional behaviour and lubricant film formation of 3D printed Ti6Al4V THR femoral heads using a pendulum hip joint simulator, which enables measurements in a realistic ball-in-cup configuration. The results were then compared with CM produced femoral head made from CoCrMo alloy and FeNiCr stainless steel. The frictional measurements comprised 10 repetitions of damped oscillatory motions, and in the majority of cases, the data exhibited high levels of reproducibility. The results for the CoCrMo and FeNiCr femoral heads were found to be close together for both the UHMWPE and PMMA acetabular cups. This is primarily attributable to their same diameter of 27.98 mm, resulting in a same value of diametric clearance [40], comparable surface roughness [20] and wettability [41]. Similarly, Ti6Al4V + DLC exhibited markedly elevated friction caused by higher surface roughness and a lower value of contact angle (Fig. 3). The surface images of Ti6Al4V + DLC (Fig. 2d) revealed the presence of grooves, which were identified as the result of imperfections in the 3D printing or surface finishing process. These grooves (thus textures) have the potential to function as reservoirs for lubricants, to offer space for accumulated wear debris, to function as micro-hydrodynamic bearings, or to reduce the contact area, thereby improving friction and wear rate [42]. A number of studies have demonstrated the beneficial impact of surface grooves on THR friction [43, 44] while some studies [45] have also indicated that micro dimples do not significantly impact the friction performance of THR resembling the importance of the grooves parameters such as shape, size and their distribution on the femoral head surface. The wettability of surfaces, as characterized by contact angle measurements (Fig. 3), influences the absorption of proteins on contact surfaces, which in turn affects friction. Proteins adsorption is more prevalent on hydrophobic surfaces [46], while highly hydrophilic surface of Ti6Al4V + DLC results in limited protein adsorption, preventing the formation of a boundary protective layer.

In general, the COF values for the PMMA cup were higher than those for the UHMWPE. PMMA is an amorphous thermoplastic material that is renowned for its perfect optical clarity but often reports high COF, and thus is frequently reinforced or modified with polytetrafluoroethylene (PTFE) [47, 48] or UHMWPE [49] in order to enhance its tribological properties. Conversely, UHMWPE is a linear polymer with a high molecular weight characterized by excellent wear resistance, low friction and high impact strength [50]. Furthermore, PMMA has higher elastic modulus, which results in a smaller contact area and higher contact pressure. This, in turn, may hinder the entry of proteins into contact area, potentially influencing protein adsorption. Furthermore, the disparities in surface roughness and diametric clearance between the PMMA and UHMWPE cups should be considered. A reduction in diametric clearance results in the formation of a thicker lubricant film in contact [15]. Additionally, the effect of DLC coating on Ti6Al4V friction has been observed to differ between PMMA and UHMWPE acetabular cups. In the case of UHMWPE, the harder and rougher surface of DLC may penetrate deeper into the softer and rougher surface of UHMWPE, leading to an adhesion or abrasive wear of the cup. In contrast, penetration of DLC coated surface into the harder PMMA is less pronounced, and the friction of the rougher DLC coated surface is overcome by the uncoated Ti6Al4V, which is known to possess insufficient tribological properties [51].

The behaviour of DLC coatings applied to metal components in contact with polyethylene was described in a study by Rothammer et al. [30], in which it was demonstrated that there was an increase in the coefficient of friction after application of DLC compared to tests where a pure alloy was used. This is in agreement with the results obtained in this study (see Fig. 5), the authors attributed this to the effect of the increase in roughness after DLC application, which was also observed for the specimens tested in this study. In particular, the roughness of the femoral heads increased from about 34 to 50 nm after coating by DLC on Ti6Al4V substrate. Ranuša et al. [52] conducted a study in which they examined samples of cobalt and titanium alloy, produced by AM, with the application of DLC coating. Glass was utilised as a counterpart for the experiments, which, due to more similar properties (such as very low surface roughness and higher modulus of elasticity), can be used for PMMA closures. The results obtained from their study indicated that, during the initial phase of the experiment, the COF levels of the AM Ti6Al4V + DLC samples were notably lower compared to those of the CoCrMo samples. However, after a certain period, a stabilisation was observed, and the friction values became almost equal, which is consistent with the results (see Fig. 6), where the average COF for CoCrMo is 0.244 and for Ti6Al4V + DLC is 0.265.

The present study also highlights the role of fluorescence microscopy in elucidating the dynamics of lubricant film formation in hip replacements. The ability to directly visualize individual SF constituents under near-physiological conditions provides critical insights into the adsorption and film dynamics on the femoral head surface. The results showed that under static loading, the adsorbed albumin layer increases with each following cycle (Fig. 7), which is crucial for the formation of a boundary layer protecting the

rubbing surfaces [10], enabling further development of the lubricant film under dynamic swinging [15]. Concerning albumin adsorption, the fluorescent images revealed faster initial adsorption onto 3D printed Ti6Al4V. However, the effect was diminished when the 3D printed Ti6Al4V was further coated by DLC. The explanation is likely in the protein conformational changes [53] and significant differences in surface wettability reported above. In particular, it was found that denatured proteins rather adsorb onto hydrophobic surfaces [46]. Thus, it is suggested that the native α-helix structure of albumin tends to be denatured under static loading, leading to the enhancement of adsorbed film on hydrophobic surfaces. The results from the dynamic part of the experiment highlight the importance of the initial adsorbed film since the dynamic film thickness is the highest for the Ti6Al4V head. The up and down fluctuations are attributed to the repeated passage of protein clusters through the contact during changing the motion direction [11].

Concerning the second observed protein, γ-globulin, the static part of the test revealed different film behaviour. As shown in Fig. 8, the adsorbed layer is somewhat stable for most heads except for FeNiCr, where the adsorbed layer thickness increases. This might be due to the optimal combination of surface wettability and surface roughness properties. Even though, it must be emphasized that there might be a contribution of chemical composition, as the aforementioned properties do not significantly differ from CoCrMo and Ti6AL4V heads. Thus, a spectroscopic analysis might better reveal the adsorption mechanisms of γ-globulin, motivating future research. The swinging part of the test showed that the film is rather constant or slightly decreases for CoCrMo, FeNiCr and Ti6Al4V + DLC heads, while an increase is observed for Ti6Al4V. Therefore, there is a close link to protein form, as γ-globulin is of β-sheet structure in a native form [53], and it was also observed before that its ability to form a stable lubricating film under motion is a bit limited [4, 18].

The last set of fluorescent observations was performed with stained HA. In this case, the variance in results was the least apparent out of the investigated constituents. Under the static test, there is a slight increase in adsorbed HA film (Fig. 9); however, it is not as significant as in the case of albumin and moreless comparable to the results of γ-globulin. Similar behaviour of all the tested heads regarding the formation of HA film is also identified during the swinging motion, where the only worth-mentioning difference may be seen for Ti6Al4V.

To sum up, it should be highlighted that pure Ti6Al4V has a very positive impact on lubricant film formation. However, concerning the expected elevated wear of Ti6Al4V under rubbing conditions [54], additional coating with DLC seems necessary. Thus, the overall biotribological performance is in finding the optimal balance between lubrication and associated wear performance. Therefore, long-term wear tests are planned as the next step when assessing the potential involvement of additively manufactured implants in a broader use. While additive manufacturing offers unique customization and surface engineering opportunities, the findings also reveal challenges. The irregularities inherent to the process, such as localized asperities, can disrupt lubricant film formation, leading to adverse wear mechanisms. These challenges emphasize the importance of optimizing post-processing techniques to minimize surface imperfections.

4.2 Limitations

The authors realize that the present study lacks several limitations. First of all, it must be emphasized that the experiments were carried out under a static load of 532 N, while under various daily activities, the load of the joints differs considerably during the cycle. However, it must be noted that the pendulum simulator does not allow control of the load during operation, as the dead weight causes the vertical load. The main benefit of this approach is that it considers realistic conformal conditions, which are found to be more critical than load variance [14].

Further concern might be related to limited statistical evidence. In this regard, it is worth mentioning that the cups for testing are costly, and multiple repetitions of a wide range of measurements are simply impossible. However, the authors gained significant experience with these tests before [14–18, 55] and established very strict experimental protocols which must be followed to come up with reliable data. When there is doubt about the experiment's progress, sample quality or any inconsistency in data evaluation, the experiment is excluded from the data set and is repeated with new samples under given conditions.

Another limitation might also be identified in the reversed arrangement of the hip joint model, where the head is placed at the top. However, this is the only option that enables (i) friction monitoring due to natural damping of the pendulum arm and (ii) simultaneous in-situ contact observation using optical methods under fully flooded conditions. If the joint arrangement were in a physiological setup (cup on top), the whole couple would have to be covered by some sleeve to avoid fluid leakage, which would disable contact observation. It is nevertheless believed that this experimental limitation should not cause significant discrepancies, as the joint in the body is encapsulated, and the synovial fluid fills the whole joint gap; thus, the contact also operates under a fully flooded regime.

Next, the variance in cup materials should be discussed briefly. As mentioned above, the present study employed UHMWPE, PMMA and glass acetabular cups. The motivation for using three different materials is in the abilities

of the applied techniques and the intention to come up with reliable, clinically relevant data. UHWMPE is a typical representative of cups used dominantly in practice; it was, therefore, used to assess the frictional performance of the tested cups. However, it is not transparent, so direct contact imaging is not possible. For that reason, the original cup was substituted by PMMA for fluorescence imaging, as PMMA is identified as a soft-matter material with mechanical properties close to the UHMWPE with sufficient optical transparency [17, 56]. The optical glass was then used due to the limitations of optical interferometry described in the below paragraph.

Last but not least, it needs to be highlighted that the comprehensive fluorescent observations resulted in a qualitative assessment of the lubricant film thickness. The literature showed that there is a linear dependence between the fluorescent intensity and film thickness; therefore, the higher intensity, the proportionally thicker lubricating film [57, 58]. Apparently, the authors were also quite interested in a quantitative assessment of film thickness. For this purpose, optical interferometry was previously successfully adopted [14, 18]. The biggest limitation is that the counterface must be made from glass (or sapphire) and additionally coated with a thin chromium layer to enhance interference of fringes and allow precise film thickness evaluation. Following previous experience, the authors performed the film thickness measurements, as can be seen in Fig. 10. In contrast to the fluorescent measurement, film thickness was analysed only for the CoCrMo and Ti6Al4V femoral heads. In order to reduce the quantity of glass acetabular cups required for the experiments, measurements with FeNiCr and Ti6Al4V + DLC were not conducted. Especially in the case of Ti6Al4V + DLC, it was anticipated that delamination of the chromium layer and scratching of the glass surface would occur due to the rough and hard surface of the femoral head. It should be noted that the primary objective was to undertake an analysis of conventionally and additively manufactured femoral heads, which was still achieved for CoCrMo and uncoated Ti6Al4V. Nevertheless, some interesting findings are still coming from this analysis, specifically in terms of pretty good film formation ability in the case of the Ti6Al4V head, which is in good compliance with fluorescent observations. Titanium head formed even thicker films than commercial CoCrMo, which was found to be very film-supportive in our previous research [15]. The authors conclude that the data from optical interferometry have rather a supportive character and do not represent the most reliable findings of the present study. For better film thickness assessment in a quantitative way, another measurement technique would have to be adopted.

5 Conclusions

In conclusion, this study has identified several key findings regarding the surface properties, friction, and lubricant film formation of additively manufactured THRs from Ti6Al4V alloy. A pendulum hip joint simulator, in conjunction with fluorescent microscopy and optical interferometry apparatus, was utilized to analyse COF and film thickness in a realistic ball-in-cup configuration, while the results of 3D printed femoral heads were compared with those of conventionally manufactured femoral heads. The main conclusions are presented below:

- The additively manufactured Ti6Al4V head showed better protein adsorption and a faster increase in lubricant film thickness, which could potentially contribute to a reduction in contact surface wear. However, concerning the expected elevated wear of Ti6Al4V, an additional surface coating seems to be necessary.
- Additive manufacturing enables the creation of surfaces with specific imperfection such as uneven surfaces or the presence of pores or dents. These imperfections can enhance the formation of the lubricant film and, subsequently, reduce friction or wear in the THR. Nevertheless, the beneficial impact of these features has not been definitively established.
- Despite exhibiting higher surface roughness, the friction of additively manufactured femoral heads was found to be comparable to that of conventionally manufactured femoral heads.
- The application of DLC coating did not result in a smoother surface of the femoral head, likely due to uneven adhesion and existing surface irregularities. The application of DLC coating also resulted in an increase in friction and a reduction in protein and HA adsorption under certain conditions.

Additive manufacturing, one of the most promising and advanced technologies of the past few decades, has become a significant part of the orthopaedical implant industry, offering undeniable benefits, while also presenting specific aspects related to the process. Surface imperfections, such as pores or dents, have the potential to affect the longevity and performance of the implant. Therefore, unintentional as well es intentional surface texturing of 3D printed femoral heads should be further investigated. These surface imperfections, particularly in the case of Ti6Al4V alloy, are also associated with a need for better surface finishing techniques, which would result in the creation of smoother rubbing surfaces. The application of DLC coating appears to be a promising method for enhancing the wear resistance of Ti6Al4V. However, in

our case, the application of DLC coating resulted in an increase in surface roughness, higher friction and a worsening of protein adsorption. Therefore, an alternative coating to improve Ti6Al4V wear should be examined as well. Lastly, the tribological properties of titanium alloys could be enhanced by the new generations of additively manufactured titanium alloys, such as Ti–Nb–Ta–Zr or Ti–Mo, Ti–Nb–Zr–Sn, which have been shown to exhibit improved biocompatibility and Young's moduli that are closer to those of human bones.

Author Contributions DR and MV conceived the idea. DR and MV designed the experiments. DR and SU performed the experiments and analysed the data. DR, LO and DN wrote the original draft of the manuscript. MV administrated the project, secured the funding, and supervised the study.

Funding Open access publishing supported by the institutions participating in the CzechELib Transformative Agreement. This research was carried out as a part of the project "Friction and lubrication of small joint implants produced by 3D metal printing additive technology", funded by the Czech Science Foundation (grant number 22-02154S), and also supported by the project "Mechanical Engineering of Biological and Bio-inspired Systems," funded as Project No. CZ.02.01.01/00/22_008/0004634 by Programme Johannes Amos Commenius, Call Excellent Research, administered by the Ministry of Education, Sports and Youth.

Data Availability The data that support the findings of this study are openly available in repository Zenodo at https://doi.org/10.5281/zenodo.15235279.

Declarations

Competing interests The authors declare no competing interests.

References

1. Evans, J.T., Evans, J.P., Walker, R.W., Blom, A.W., Whitehouse, M.R., Sayers, A.: How long does a hip replacement last? A systematic review and meta-analysis of case series and national registry reports with more than 15 years of follow-up. Lancet (2019). https://doi.org/10.1016/S0140-6736(18)31665-9
2. Linder, R., Müller, H., Grenz-Farenholtz, B., Wagner, C., Stockheim, M., Verheyen, F.: Replacement of endoprosthetic implants within a two years follow-up period: a statutory health insurance routine data analysis. BMC Musculoskelet. Disord. (2012). https://doi.org/10.1186/1471-2474-13-223
3. Bayliss, L.E., Culliford, D., Monk, A.P., Glyn-Jones, S., Prieto-Alhambra, D., Judge, A., Cooper, C., Carr, A.J., Arden, N.K., Beard, D.J., Price, A.J.: The effect of patient age at intervention on risk of implant revision after total replacement of the hip or knee: a population-based cohort study. Lancet **389**, 1424–1430 (2017). https://doi.org/10.1016/S0140-6736(17)30059-4
4. Nečas, D., Vrbka, M., Urban, F., Křupka, I., Hartl, M.: The effect of lubricant constituents on lubrication mechanisms in hip joint replacements. J. Mech. Behav. Biomed. Mater. **55**, 295–307 (2016). https://doi.org/10.1016/j.jmbbm.2015.11.006
5. Gallo, J., Goodman, S.B., Konttinen, Y.T., Raska, M.: Particle disease: biologic mechanisms of periprosthetic osteolysis in total hip arthroplasty. Innate Immun. **19**, 213–224 (2013). https://doi.org/10.1177/1753425912451779
6. Cross, M.B., Nam, D., Mayman, D.J.: Ideal Femoral head size in total hip arthroplasty balances stability and volumetric wear. HSS J. **8**, 270–274 (2012). https://doi.org/10.1007/s11420-012-9287-7
7. Mavraki, A., Cann, P.M.: Friction and lubricant film thickness measurements on simulated synovial fluids. Proc. Inst. Mech. Eng. Part J **223**, 325–335 (2009). https://doi.org/10.1243/13506501JET580
8. Mavraki, A., Cann, P.M.: Lubricating film thickness measurements with bovine serum. Tribol. Int. **44**, 550–556 (2011). https://doi.org/10.1016/j.triboint.2010.07.008
9. Fan, J., Myant, C.W., Underwood, R., Cann, P.M., Hart, A.: Inlet protein aggregation. Proc. Inst. Mech. Eng. Part H **225**, 696–709 (2011). https://doi.org/10.1177/0954411911401306
10. Myant, C., Underwood, R., Fan, J., Cann, P.M.: Lubrication of metal-on-metal hip joints: the effect of protein content and load on film formation and wear. J. Mech. Behav. Biomed. Mater. **6**, 30–40 (2012). https://doi.org/10.1016/j.jmbbm.2011.09.008
11. Myant, C.W., Cann, P.: The effect of transient conditions on synovial fluid protein aggregation lubrication. J. Mech. Behav. Biomed. Mater. **34**, 349–357 (2014). https://doi.org/10.1016/j.jmbbm.2014.02.005
12. Myant, C., Cann, P.: On the matter of synovial fluid lubrication: implications for metal-on-metal hip tribology. J. Mech. Behav. Biomed. Mater. **34**, 338–348 (2014). https://doi.org/10.1016/j.jmbbm.2013.12.016
13. Vrbka, M., Křupka, I., Hartl, M., Návrat, T., Gallo, J., Galandáková, A.: In situ measurements of thin films in bovine serum lubricated contacts using optical interferometry. Proc. Inst. Mech. Eng. Part H (2014). https://doi.org/10.1177/0954411913517498
14. Vrbka, M., Nečas, D., Hartl, M., Křupka, I., Urban, F., Gallo, J.: Visualization of lubricating films between artificial head and cup with respect to real geometry. Biotribology **1–2**, 61–65 (2015). https://doi.org/10.1016/j.biotri.2015.05.002
15. Nečas, D., Vrbka, M., Urban, F., Gallo, J., Křupka, I., Hartl, M.: In situ observation of lubricant film formation in THR considering real conformity: the effect of diameter, clearance and material. J. Mech. Behav. Biomed. Mater. **69**, 66–74 (2017). https://doi.org/10.1016/j.jmbbm.2016.12.018
16. Nečas, D., Vrbka, M., Rebenda, D., Gallo, J., Galandáková, A., Wolfová, L., Křupka, I., Hartl, M.: In situ observation of lubricant film formation in THR considering real conformity: the effect of model synovial fluid composition. Tribol. Int. **117**, 206–216 (2018). https://doi.org/10.1016/j.triboint.2017.09.001
17. Nečas, D., Vrbka, M., Galandáková, A., Křupka, I., Hartl, M.: On the observation of lubrication mechanisms within hip joint replacements. Part I: Hard-on-soft bearing pairs. J. Mech. Behav. Biomed. Mater. **89**, 237–248 (2019). https://doi.org/10.1016/j.jmbbm.2018.09.022

18. Nečas, D., Vrbka, M., Gallo, J., Křupka, I., Hartl, M.: On the observation of lubrication mechanisms within hip joint replacements. Part II: Hard-on-hard bearing pairs. J. Mech. Behav. Biomed. Mater. **89**, 249–259 (2019). https://doi.org/10.1016/j.jmbbm.2018.09.026
19. Vrbka, M., Návrat, T., Křupka, I., Hartl, M., Šperka, P., Gallo, J.: Study of film formation in bovine serum lubricated contacts under rolling/sliding conditions. Proc. Inst. Mech. Eng. Part J. **227**, 459–475 (2013). https://doi.org/10.1177/1350650112471000
20. Vrbka, M., Nečas, D., Bartošík, J., Hartl, M., Křupka, I., Galandáková, A., Gallo, J.: Determination of a friction coefficient for THA bearing couples. Acta Chir. Orthop. Traumatol. Cechoslov. **82**, 341–347 (2015). https://doi.org/10.55095/achot2015/057
21. Nečas, D., Vrbka, M., Křupka, I., Hartl, M.: The effect of kinematic conditions and synovial fluid composition on the frictional behaviour of materials for artificial joints. Materials **11**, 767 (2018). https://doi.org/10.3390/ma11050767
22. Narra, S.P., Mittwede, P.N., DeVincent Wolf, S., Urish, K.L.: Additive manufacturing in total joint arthroplasty. Orthop. Clin. N. Am. **50**, 13–20 (2019). https://doi.org/10.1016/j.ocl.2018.08.009
23. Khal, A.-A., Apostu, D., Schiau, C., Bejinariu, N., Pesenti, S., Jouve, J.-L.: Custom-made 3D-printed prosthesis after resection of a voluminous giant cell tumour recurrence in Pelvis. Diagnostics (2023). https://doi.org/10.3390/diagnostics13030485
24. Ran, Q., Yang, W., Hu, Y., Shen, X., Yu, Y., Xiang, Y., Cai, K.: Osteogenesis of 3D printed porous Ti6Al4V implants with different pore sizes. J. Mech. Behav. Biomed. Mater. **84**, 1–11 (2018). https://doi.org/10.1016/j.jmbbm.2018.04.010
25. Grosse, S., Haugland, H.K., Lilleng, P., Ellison, P., Hallan, G., Høl, P.J.: Wear particles and ions from cemented and uncemented titanium-based hip prostheses—a histological and chemical analysis of retrieval material. J. Biom. Mater. Res. Part B **103**, 709–717 (2015). https://doi.org/10.1002/jbm.b.33243
26. Odehnal, L., Ranuša, M., Vrbka, M., Křupka, I., Hartl, M.: Tribological behaviour of Ti6Al4V alloy: an application in small joint implants. Tribol. Lett. (2023). https://doi.org/10.1007/s11249-023-01795-4
27. Bartolomeu, F., Buciumeanu, M., Pinto, E., Alves, N., Silva, F.S., Carvalho, O., Miranda, G.: Wear behavior of Ti6Al4V biomedical alloys processed by selective laser melting, hot pressing and conventional casting. Trans. Nonferrous Met. Soc. China **27**, 829–838 (2017). https://doi.org/10.1016/S1003-6326(17)60060-8
28. Goyal, V., Verma, G.: Tribological behavior of direct metal laser sintering-manufactured Ti6Al4V alloy in different biofluids for orthopedic implants. J. Tribol. (2024). https://doi.org/10.1115/1.4064506
29. Skjöldebrand, C., Tipper, J.L., Hatto, P., Bryant, M., Hall, R.M., Persson, C.: Current status and future potential of wear-resistant coatings and articulating surfaces for hip and knee implants. Mater. Today Bio. (2022). https://doi.org/10.1016/j.mtbio.2022.100270
30. Rothammer, B., Neusser, K., Bartz, M., Wartzack, S., Schubert, A., Marian, M.: Evaluation of the wear-resistance of DLC-coated hard-on-soft pairings for biomedical applications. Wear (2023). https://doi.org/10.1016/j.wear.2023.204728
31. Thorwarth, K., Thorwarth, G., Figi, R., Weisse, B., Stiefel, M., Hauert, R.: On interlayer stability and high-cycle simulator performance of diamond-like carbon layers for articulating joint replacements. Int. J. Mol. Sci. **15**, 10527–10540 (2014). https://doi.org/10.3390/ijms150610527
32. de Oliveira, L.Y.S., Siqueira, C.J.M., Fernandes, B.L., Kuromoto, N., Retraint, D.: Wear behavior of diamond-like carbon deposited on Ti6Al4V prepared with surface mechanical attrition treatment. Mater. Res. (2019). https://doi.org/10.1590/1980-5373-mr-2018-0568
33. Xie, D., Liu, H., Deng, X., Leng, Y.X., Huang, N.: Deposition of a-C: H films on UHMWPE substrate and its wear-resistance. Appl. Surf. Sci. **256**, 284–288 (2009). https://doi.org/10.1016/j.apsusc.2009.08.017
34. Puértolas, J.A., Martínez-Nogués, V., Martínez-Morlanes, M.J., Mariscal, M.D., Medel, F.J., López-Santos, C., Yubero, F.: Improved wear performance of ultra high molecular weight polyethylene coated with hydrogenated diamond like carbon. Wear **269**, 458–465 (2010). https://doi.org/10.1016/j.wear.2010.04.033
35. Rothammer, B., Neusser, K., Marian, M., Bartz, M., Krauß, S., Böhm, T., Thiele, S., Merle, B., Detsch, R., Wartzack, S.: Amorphous carbon coatings for total knee replacements—Part I: deposition, cytocompatibility, chemical and mechanical properties. Polymers **13**, 1952 (2021). https://doi.org/10.3390/polym13121952
36. Rothammer, B., Marian, M., Neusser, K., Bartz, M., Böhm, T., Krauß, S., Schroeder, S., Uhler, M., Thiele, S., Merle, B., Kretzer, J.P., Wartzack, S.: Amorphous carbon coatings for total knee replacements—Part II: tribological behavior. Polymers **13**, 1880 (2021). https://doi.org/10.3390/polym13111880
37. Rothammer, B., Schwendner, M., Bartz, M., Wartzack, S., Böhm, T., Krauß, S., Merle, B., Schroeder, S., Uhler, M., Kretzer, J.P., Weihnacht, V., Marian, M.: Wear mechanism of superhard tetrahedral amorphous carbon (ta-C) coatings for biomedical applications. Adv. Mater. Interfaces **10**, 2202370 (2023). https://doi.org/10.1002/admi.202202370
38. Galandáková, A., Ulrichová, J., Langová, K., Hanáková, A., Vrbka, M., Hartl, M., Gallo, J.: Characteristics of synovial fluid required for optimization of lubrication fluid for biotribological experiments. J. Biomed. Mater. Res. Part B **105**, 1422–1431 (2017). https://doi.org/10.1002/jbm.b.33663
39. Crisco, J.J., Blume, J., Teeple, E., Fleming, B.C., Jay, G.D.: Assuming exponential decay by incorporating viscous damping improves the prediction of the coeffcient of friction in pendulum tests of whole articular joints. Proc. Inst. Mech. Eng. Part H (2007). https://doi.org/10.1243/09544119JEIM248
40. Brockett, C.L., Harper, P., Williams, S., Isaac, G.H., Dwyer-Joyce, R.S., Jin, Z., Fisher, J.: J. Mater. Sci. Mater. Med. **19**, 1575–1579 (2008). https://doi.org/10.1007/s10856-007-3298-9
41. Zhang, C., Fujii, M.: Influence of wettability and mechanical properties on tribological performance of DLC coatings under water lubrication. J. Surf. Eng. Mater. Adv. Technol. **05**, 110–123 (2015). https://doi.org/10.4236/jsemat.2015.53013
42. Allen, Q., Raeymaekers, B.: Surface texturing of prosthetic hip implant bearing surfaces: a review. J. Tribol. (2021). https://doi.org/10.1115/1.4048409
43. Tewelde, F.B., Allen, Q., Zhou, T.: Multiscale texture features to enhance lubricant film thickness for prosthetic hip implant bearing surfaces. Lubricants (2024). https://doi.org/10.3390/lubricants12060187
44. Nečas, D., Usami, H., Niimi, T., Sawae, Y., Křupka, I., Hartl, M.: Running-in friction of hip joint replacements can be significantly reduced. Friction **8**, 1137–1152 (2020). https://doi.org/10.1007/s40544-019-0351-x
45. Choudhury, D., Ay Ching, H., Mamat, A.B., Cizek, J., Abu Osman, N.A., Vrbka, M., Hartl, M., Krupka, I.: Fabrication and characterization of DLC coated microdimples on hip prosthesis heads. J. Biomed. Mater. Res. Part B (2015). https://doi.org/10.1002/jbm.b.33274
46. Heuberger, M.P., Widmer, M.R., Zobeley, E., Glockshuber, R., Spencer, N.D.: Protein-mediated boundary lubrication in arthroplasty. Biomaterials **26**, 1165–1173 (2005). https://doi.org/10.1016/j.biomaterials.2004.05.020
47. Gu, D., Zhang, L., Chen, S., Song, K., Liu, S.: Significant reduction of the friction and wear of PMMA based composite by

filling with PTFE. Polymers (2018). https://doi.org/10.3390/polym10090966
48. Peng, S., Zhang, L., Xie, G., Guo, Y., Si, L., Luo, J.: Friction and wear behavior of PTFE coatings modified with poly (methyl methacrylate). Compos. B **172**, 316–322 (2019). https://doi.org/10.1016/j.compositesb.2019.04.047
49. Gu, D., Wang, S., Zhang, J., Liu, K., Chen, S., Chen, X., Wang, Z., Liu, J.: Improved tribological properties of Poly(methyl methacrylate) based composites by the synergistic effect of incorporating ultra-high molecular weight polyethylene and heat treatment. J. Mater. Eng. Perform. (2022). https://doi.org/10.1007/s11665-022-06638-2
50. Merola, M., Affatato, S.: Materials for hip prostheses: a review of wear and loading considerations. Materials (2019). https://doi.org/10.3390/ma12030495
51. Philip, J.T., Mathew, J., Kuriachen, B.: Tribology of Ti6Al4V: a review. Friction. **7**, 497–536 (2019). https://doi.org/10.1007/s40544-019-0338-7
52. Ranuša, M., Čípek, P., Vrbka, M., Paloušek, D., Křupka, I., Hartl, M.: Tribological behaviour of 3D printed materials for small joint implants: a pilot study. J. Mech. Behav. Biomed. Mater. (2022). https://doi.org/10.1016/j.jmbbm.2022.105274
53. Nečas, D., Sawae, Y., Fujisawa, T., Nakashima, K., Morita, T., Yamaguchi, T., Vrbka, M., Křupka, I., Hartl, M.: The influence of proteins and speed on friction and adsorption of metal/UHMWPE contact pair. Biotribology **11**, 51–59 (2017). https://doi.org/10.1016/j.biotri.2017.03.003
54. Katti, K.S., Verma, D., Katti, D.R.: Materials for joint replacement. Joint replacement technology, pp. 81–104 (2008). https://doi.org/10.1533/9781845694807.1.81
55. Lu, X., Nečas, D., Meng, Q., Rebenda, D., Vrbka, M., Hartl, M., Jin, Z.: Towards the direct validation of computational lubrication modelling of hip replacements. Tribol. Int. (2020). https://doi.org/10.1016/j.triboint.2020.106240
56. Nečas, D., Vrbka, M., Marian, M., Rothammer, B., Tremmel, S., Wartzack, S., Galandáková, A., Gallo, J., Wimmer, M.A., Křupka, I., Hartl, M.: Towards the understanding of lubrication mechanisms in total knee replacements – Part I. Tribol. Int. (2021). https://doi.org/10.1016/j.triboint.2021.106874
57. Azushima, A.: In lubro 3D measurement of oil film thickness at the interface between tool and workpiece in sheet drawing using a fluorescence microscope. Tribol. Int. **38**, 105–112 (2005). https://doi.org/10.1016/j.triboint.2004.04.006
58. Azushima, A.: In situ 3D measurement of lubrication behavior at interface between tool and workpiece by direct fluorescence observation technique. Wear **260**, 243–248 (2006). https://doi.org/10.1016/j.wear.2005.01.053

Authors and Affiliations

David Rebenda[1,2] · Lukáš Odehnal[1] · Simona Uhrová[1] · David Nečas[1] · Martin Vrbka[1]

✉ David Rebenda
David.Rebenda@vut.cz

[1] Biotribology Research Group, Faculty of Mechanical Engineering, Brno University of Technology, Technicka 2896/2, 616 69 Brno, Czech Republic

[2] Centre of Polymer Systems, University Institute, Tomas Bata University in Zlin, Trida Tomase Bati 5678, 760 01 Zlin, Czech Republic